# Coordinated Control of Parallel Power Conditioners Synthesizing Resistive Loads in Single-Phase AC Microgrids

Augusto Matheus dos Santos Alonso[1,3], Danilo Iglesias Brandao[2], Fernando Pinhabel Marafão[1], Elisabetta Tedeschi[3]

[1]Group of Automation and Integrated Systems
Sao Paulo State University (UNESP)
Sorocaba, Brazil
augusto.alonso@unesp.br;
fernando.marafao@unesp.br

[2]Graduate Program in Electrical Engineering
Federal University of Minas Gerais (UFMG)
Belo Horizonte, Brazil
dibrandao@ufmg.br

[3]Department of Electric Power Engineering
Norwegian University of Science & Technology (NTNU)
Trondheim, Norway
elisabetta.tedeschi@ntnu.no

## Acknowledgements

The authors are grateful to the Sao Paulo Research Foundation (FAPESP) (Grants 2016/08645-9, 2017/24652-8, 2018/22172-1), CNPq (grant 420850/2016-3) and the Research Council of Norway (Grant f261735/H30).

## Keywords

Harmonics, Load sharing control, Microgrid, Parallel operation, Power conditioning.

## Abstract

Without proper coordination, power conditioners within microgrids are prone to suffer from resonance phenomena due to the complex and dynamic interactions among the main grid, nonlinear loads and distributed converters. In addition to the detriment of grid-connected devices and loads, harmonic voltage resonances may also lead to microgrid instability. As a consequence, the steering of distributed power conditioners to diminish voltage distortions and suppress undesired currents has been playing a key role on enhancing the operational stiffness of microgrids. In general, such conditioners are driven by the synthesis of sinusoidal currents independently on the status of voltage waveforms, which may not adequately damp harmonic resonances and still jeopardize system stability. Thus, this work proposes the coordination of multiple parallel power conditioners, which are driven as controlled current sources, through a current-based approach that synthesizes resistive loads, enhancing the system capability to damp voltage resonances, as well as improving power quality within microgrids. Simulation results comprising a single-phase microgrid with resonant and nonlinear loads, as well as two distributed power conditioners, are presented to demonstrate the effectiveness of the approach.

## Acronyms and Nomenclature

| | | | |
|---|---|---|---|
| CC | Central controller | $I_{nom}^{fn}$ | Nominal peak current of the *n*-th SPI |
| RLS | Resistive load synthesis | $I_h^{PCC}$ | PCC peak current at harmonic *h* |
| SLS | Sinusoidal current synthesis | $I_h^{PCC*}$ | Reference for the PCC peak current at harmonic *h* |
| SPI | Switching power interface | $I_h^L$ | Load peak current at harmonic *h* |
| $\|\|$ | Index of in-phase term | $\Delta I$ | Availability of peak current considering *N* SPIs |
| $\perp$ | Index of quadrature term | $\Delta I^n$ | Availability of peak current of the *n*-th SPI |

| | | | |
|---|---|---|---|
| $i_{local}$ | Local current of a node | $k$ | Actual control cycle of the CBC window |
| $i_a$ | Fryze's active current | $P$ | Average active power |
| $i_{na}$ | Fryze's non-active current | $v_{local}$ | Local voltage of a node |
| $i^{n*}$ | Time-domain current reference of the *n*-th SPI | $x_h$ | Unitary sinusoidal reference of harmonic $h$ |
| $I_h^*$ | Reference peak current for the *N* SPIs | $\alpha_h^*$ | Scaling coefficient broadcasted for the *N* SPIs |
| $I_h^{fn}$ | Peak current of the *n*-th SPI at harmonic $h$ | | |

# Introduction

Resonance phenomenon in electrical power systems is an important matter due to its detrimental effects on voltage quality, damaging electronics, and boosting power losses [1]. As previously discussed in literature, harmonic resonances are likely to occur in sensitive power networks, such as in offshore oil platforms [2], wind farms [3], and weak distribution systems like microgrids (MGs) [4]. Series and shunt resonances can be amplified by shunt capacitor banks and be excited by the presence of variable frequency drives, and, as recently discussed in [5], also caused by the heavy presence of other nonlinear loads. Therefore, the adoption of countermeasures to suppress such undesired issue is of great importance.

Particularly, focusing on MGs, the employment of switching power interfaces (SPIs) acting as power conditioners (active power filters (APFs), multi-functional inverters, etc.) has been playing a key role on tackling power quality issues, since they are able to dynamically adjust their operational setpoints to better meet given compensation goals [6]. Such goals are typically related to reactive power compensation and harmonic suppression, by employing SPIs operating according to many possible local control strategies [6]-[9] that, in general, perform sinusoidal current synthesis (SCS) or resistive load synthesis (RLS).

The adoption of SCS strategies is mainly due to its simplicity and low computational effort to be embedded in digital processors [7]. It provides means to obtain the circulation of sinusoidal currents in-phase with the corresponding fundamental voltages, irrespective of the voltage waveforms. However, when a distorted grid voltage condition is present, and/or resonances are excited in specific nodes within the circuit, this strategy causes the system inability to damp such harmonic voltage amplification [7]-[9]. Contrariwise, if RLS is chosen as control strategy, the resulting currents drawn by the circuit will present the same harmonics existing in the voltage waveform, not affecting the damping factor, providing suppression of resonances and increasing the power quality [6]-[9].

Yet, as the number of SPIs dispersed in MGs has been increasing considerably, more complexity is faced in terms of properly managing the entire electrical network and desired compensation goals, requiring the development of control approaches able to coordinate their operation in a reliable manner. Therefore, several decentralized and centralized control methodologies have been recently proposed to overcome this challenge [4], [10]-[15].

In general, droop control and its variations [4], [10]-[13], have been the most adopted techniques to provide coordinated control in MGs, driving SPIs as voltage-controlled sources under hierarchical topologies. They are implemented upon decentralized approaches that are independent of communication. Alternatively, a few other approaches focus on centralized topologies [14]-[15], relying on communication links to exchange information among a central/master controller and many distributed SPIs.

Following the operational concept brought by a master/slave topology, and driving SPIs as current controlled sources as depicted in Fig. 1, an alternative centralized control method for power conditioners, so-called Current-Based Control (CBC), was presented in [16] showing the ability to coordinate several parallel SPIs, allowing active, reactive and selective harmonic current sharing in MGs. With groundwork on a hierarchical control methodology, and different from other approaches [10]-[14], the CBC algorithm is fully based on the analyses of peak current terms flowing within the

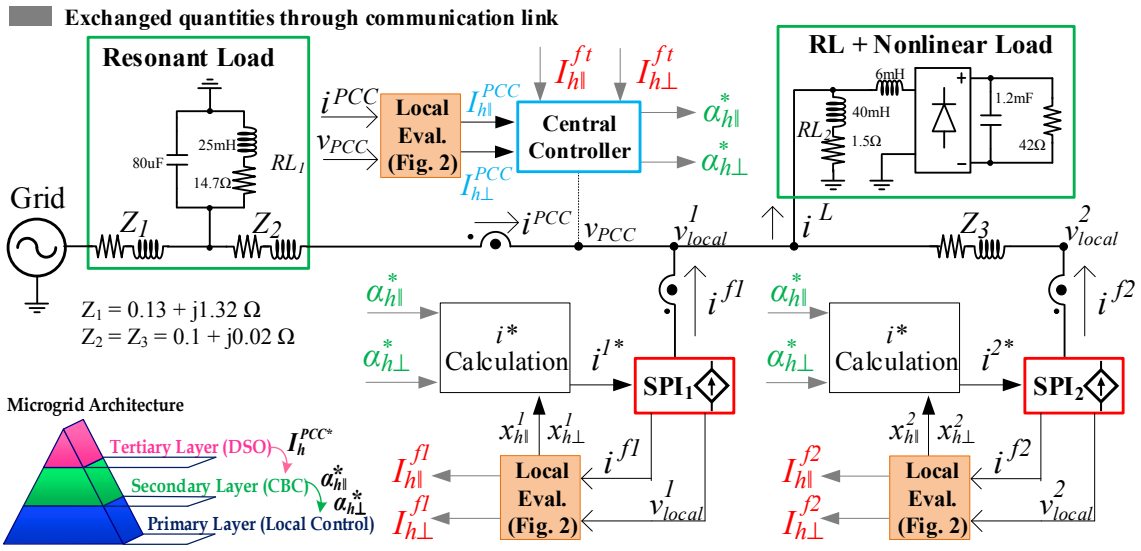


Fig. 1: Microgrid architecture and circuit adopted for simulations.

MG. It coordinates distributed conditioners proportionally, meaning that they are driven to respect their power capabilities, while balancing the thermal stress among them. Nonetheless, when set to compensate all existing harmonics (or the most significant orders), it presents an intrinsic characteristic of distributedly performing SCS, which is tied to some inconveniences as aforementioned.

Therefore, this work presents an alternative approach, employing the CBC to coordinate parallel SPIs synthesizing resistive loads within a single-phase MG. Through the insertion of the non-active current parcel defined by Fryze [17], the proposed adapted CBC approach allows RLS to be performed distributedly based on the coordination of dispersed SPIs. The method allows to maintain the system ability to damp harmonic resonances even under distorted grid conditions, increasing the power factor and improving voltage quality at the point of common coupling (PCC) in an interconnected MG, in comparison to the traditional SCS approach.

## Current-Based Control of Distributed SPIs

Based on a hierarchical approach, the CBC algorithm is placed at the secondary layer, as seen in Fig. 1, taking advantage of a master/slave architecture. In this strategy, a central controller (CC) is responsible for gathering and processing data packets from slave units (i.e., power conditioners), and then it dispatches control commands to be used locally for the synthesis of currents to be injected by each $n$ distributed SPI ($i^{n*}$). The primary control layer is responsible for the local management of such slave agents (i.e., SPI), coordinating the interaction of a SPI with the MG. This means that this lower layer is embedded in each SPI, being responsible for the synchronization with MG voltages, maintaining functionalities required for compliance with interconnection standards (i.e., anti-islanding, power factor control, volt-var capability, etc) [18]. Finally, a tertiary layer exists imposing the current references desired at the MG's PCC ($I_h^{PCC*}$), being mainly constituted from interactions with the distribution system operator (DSO) or MG manager. Based on such architecture, the coordinated current-based approach then steers distributed power conditioners, aiming to compensate non-active current terms, on the basis of the three following steps, which are: the local evaluation of electrical quantities, the gathering of current terms from SPIs at the CC, and the generation of local current references for the SPIs.

*1. Local evaluation of electrical quantities*

Considering a single-phase approach, the first step of the CBC method is determined by the local evaluation of electrical quantities, as seen in Fig. 2. The local (respective to PCC or SPIs' nodes) current and voltage are measured, whereas the voltage is used in a time-domain approach based on a phase-locked loop (PLL) algorithm, which allows the identification of in-phase and quadrature terms for a set of $H$ selected harmonic frequencies. Although the PLL methodology presented in [19] is herein adopted, any other approaches could be integrated to the method as well.

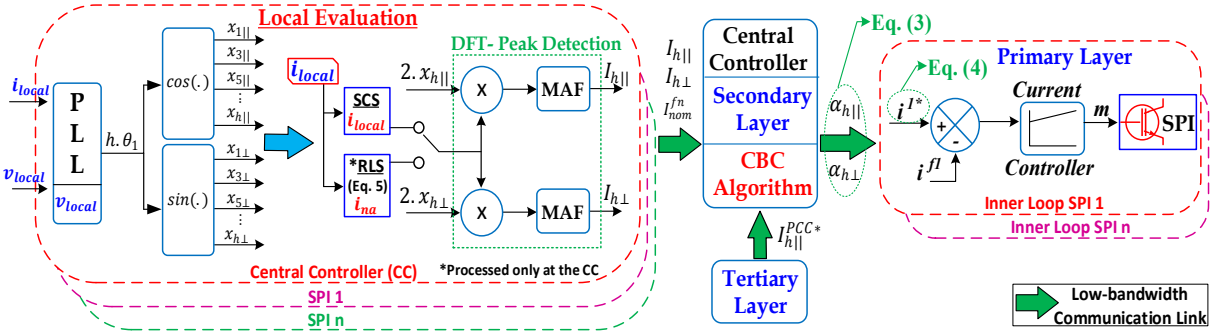


Fig. 2: Local evaluation of electrical quantities and reference current generation for SPIs with the CBC performing SCS or RLS.

After that stage, the respective in-phase and quadrature reference signals, $x_{h||}$ and $x_{h\perp}$, are generated to attain unitary waveform references in relation to each nodal voltage ($v_{local}$). Such references, after being multiplied by the local current $i_{local}$ (i.e., $i_{local} = i^{f1}$, $i^{f2}$ or $i^{PCC}$), are processed by a Discrete Fourier Transform (DFT) implemented through moving average filters (MAFs), aiming at detecting the magnitudes (i.e, peak values) of the in-phase and quadrature currents, $I_{h||}$ and $I_{h\perp}$, for each $h$ harmonic order (including the fundamental component, i.e. $h \geq 1$, considering only odd orders). Note that, as seen in Fig. 1, $i^{fn}$ and $i^{PCC}$ stand for the time-domain currents being, respectively, injected by the $n$-th power conditioner, and drawn from the mains. Yet, since this work focuses on power conditioners (i.e., not processing the sharing of active currents), during the current decomposition proposed by the CBC, the fundamental in-phase current term ($I_{1||}$) is neglected by the algorithm; only the terms $I_{1\perp}$, $I_{h||}$ and $I_{h\perp}$ (for a set of $H$ harmonic orders) are processed.

*2. Gathering current terms from SPIs*

Upon completing the calculation of the peak currents at each node where a participating SPI is placed, the second step of the CBC algorithm starts by using a low-bandwidth communication link to gather such information at the CC. Such terms of current magnitudes injected by each $n$-th SPI, along with their nominal current capability, $I_{nom}^{fn}$, are then gathered on a data packet and transmitted to the CC, where the secondary layer and CBC algorithm are processed. In addition, since the CC is placed at the PCC as shown in Fig. 1, the local evaluation of the electrical quantities at this node is processed directly by it. Knowing that the CC possesses the current terms being injected by the SPIs in the actual control cycle $k$, by referring to Fig. 1 and considering that voltage phase deviation in a low-voltage scenario is practically neglected among MG's nodes, one can note that by Kirchhoff's current law, the load currents are given by the sum of currents from the SPIs plus the PCC as in (1). Thus, as given by (2), the CC can compute the MG current reference ($I_h^*$) for the next control cycle, considering all desired in-phase and quadrature harmonic orders (plus the fundamental in-quadrature component), required to provide load sharing among SPIs.

$$I_h^L(k) = I_h^{PCC}(k) + \sum_{n=1}^{N} I_h^{fn}(k) \tag{1}$$

$$I_h^*(k+1) = I_h^L(k) - I_h^{PCC*}(k+1) = I_h^{PCC}(k) + \sum_{n=1}^{N} I_h^{fn}(k) - I_h^{PCC*}(k+1) \tag{2}$$

Afterwards, since the CC also knows the nominal current capabilities of all SPIs (i.e., the overall amount available on the MG, namely $\Delta I$), it can calculate scaling coefficients, $\alpha_{h||}$ and $\alpha_{h\perp}$, that balance the participation of all converters participating on the current sharing, according to their current limitations as given by (3). $\alpha_{h||}$ and $\alpha_{h\perp}$ are calculated for each $h$ harmonic order aimed to be controlled at the MG, being processed sequentially. They are positive or negative according to the desired regulation of current parcels (e.g., $\alpha_{1\perp}$ controls reactive current circulation and it is positive for regulation of inductive currents, or it counteracts capacitive behavior if negative). Yet, also note that $\Delta I$

is initially given by the square of the sum of $I_{nom}^{fn}$ considering all *n*, and it must be recalculated after the allocation of each $\alpha_h$ term to avoid overcurrents, which is done by orthogonal subtractions, since quadrature harmonic current terms are processed after in-phase terms. Then, the CC is finally responsible for dispatching such control coefficients to SPIs through the communication link following a broadcasting approach.

$$\alpha_{h||} = \frac{I_{h||}^{*}(k+1)}{\sqrt{\Delta I}} \qquad and \qquad \alpha_{h\perp} = \frac{I_{h\perp}^{*}(k+1)}{\sqrt{\Delta I}} \tag{3}$$

*3. Generation of local current references*

The third and last stage comprises the processing of the broadcasted scaling coefficients at the primary layer of each SPI. This step comprises the means for attaining the final reference current to be injected by each SPI. As represented in Fig. 1, such coefficients are used locally by a SPI to calculate the time-domain current ($i^{n*}$), which is used to control the power conditioners and their respective contribution to the expected load sharing. Such control reference is attained by (4), on which $\Delta I^n$ represents the local current availability, being recalculated recursively as each harmonic order is accounted for in the generation of the current $i^{n*}$. Again, it is reinforced that $\alpha_{1||}$ is null and consequentially it is neither calculated at the CC nor computed by power conditioners, since the latter do not present the capability to process active power. $i^{n*}$ is then compared to the SPI injected current and used within the inner current loop controller.

$$i^{n*} = \sum_{h=1,3,5,\dots}^{H} \left[\left(\alpha_{h||}.\sqrt{\Delta I^n}\right).x_{h||}^{n} + \left(\alpha_{h\perp}.\sqrt{\Delta I^n}\right).x_{h\perp}^{n}\right] \tag{4}$$

# Coordinated Current-Based Control of Distributed SPIs Performing RLS

Due to the feature of using unitary sinusoidal references (i.e., $x_{h||}$ and $x_{h\perp}$) on the synthesis of control references for the SPIs currents as in (4), the CBC methodology inherently provides distributed compensation of load currents being characterized by an SCS approach. This means that, upon steering SPIs to share undesired currents flowing at the PCC (i.e., the most significant harmonic parcels), the remaining current is ideally sinusoidal and in-phase with voltages, regardless of the voltage waveform. Therefore, on a scenario of highly distorted voltages occurring from harmonic resonances over the MG, the damping capability of the system is reduced on the classic implementation of the CBC algorithm.

On the contrary, if a RLS approach is intended to be applied to the distributed operation of power conditioners, the CBC can be flexibly adapted by replacing the instantaneous measured current, $i_{local}$, by its non-active current term ($i_{na}$) as depicted in Fig. 2. Such non-active parcel, considering a single-phase system, is given by (5), in which the Fryze's active current parcel ($i_a$) is subtracted from the local total current.

$$i_{na} = i_{local} - i_a = i_{local} - \frac{P}{V^2}.v_{local} \tag{5}$$

Such time-domain active current, $i_a$, is defined from the relation of the average active power ($P$) of the node, the rms value ($V$) and instantaneous waveform ($v_{local}$) of the nodal voltage. For this RLS method, the fundamental in-phase current term ($I_{1||}$) decomposed by the CBC from $i_{na}$ is already null, due to the fact that $i_{na}$ does not convey active current. As a consequence, by steering conditioners to share load currents while only compensating the non-active current term $i_{na}$, it results in PCC currents that ideally present the same waveform of voltages and harmonics following the same proportions; therefore, the harmonic voltage damping of the system can be consequently enhanced [6,7] upon incidence of resonances. It is also reinforced that this adjustment on the classic CBC algorithm [15] is only required to be implemented on the nodal evaluation occurring at the PCC, which is realized by the CC. SPIs can maintain their operation by decomposing $i_{local}$ without impairing in inconsistencies with Kirchhoff's current law.

Another important remark is that the CBC is a selective approach for distributed control, targeting specific harmonic terms (e.g., in the later presented simulation cases, the fundamental, 3rd, 5th and 7th

orders). Therefore, while performing SCS, it provides the compensation of harmonics, regardless of the voltage waveform, focusing only on those specific orders set, and not on the entire harmonic spectrum of $i_{local}$. On the contrary, although the RLS approach is similarly selective, by decomposing $i_{na}$, it only compensates the reactive and harmonic parcels not responsible for transferring active power.

## Simulation Cases of RLS and SCS in a Single-Phase Microgrid

To evaluate the distributed RLS and SCS methodologies in a single-phase low-voltage MG, a circuit with two distributed SPIs is adopted, following the same scheme previously shown in Fig. 1. In addition to the 60 Hz fundamental voltage with magnitude of 127 $V_{rms}$, a small distortion of 2 % of 5$^{th}$ harmonic is added to the grid voltage to excite a resonant load placed at the PCC of the MG. Such resonant load comprises the line impedances $Z_1$ and $Z_2$, and a capacitor bank calculated to compensate the reactive power of the existing $RL_1$ load. Another nonlinear load is also present on the MG in parallel to a second $RL_2$ load to worsen current and voltage distortions. Power conditioners, driven as controlled current sources, are emulated by full-bridge SPIs with LCL output filters (with grid and SPI side inductors equal to 1.0 mH, capacitor of 3.3 $\mu$F and passive damping resistor of 2.0 Ω), being modulated by three-level PWMs. Switching frequency is 12 kHz and constant voltage sources of $V_{DC}$ = 235 V are placed at the DC bus of the SPIs. The inner current loop of SPIs uses proportional-resonant (PRes) controllers designed as in [20], tuned for the fundamental, plus 3$^{rd}$, 5$^{th}$ and 7$^{th}$ harmonics. PSIM software is used for simulations.

The CBC algorithm is set to coordinate SPIs for the compensation of fundamental reactive currents ($i_{1\perp}$), and also to suppress current harmonics (in-phase and quadrature) from the 3$^{rd}$, 5$^{th}$, and 7$^{th}$ orders. A transmission rate of 16.66 ms is chosen for the control packets and local information to flow among the CC and the two active power conditioners. $SPI_1$ presents a nominal peak current value of $I_{nom}^{f1}$ = 10.0 A, and for the other SPI, it is $I_{nom}^{f2}$ = 6.0 A, which results in a proportion ratio of $r_{SPIs} = 10/6 = 1.66$. The DSO peak current reference ($I_h^{PCC*}$), which determines the desired current flow at PCC, is set to be null for the abovementioned harmonic orders adopted, as well as for the quadrature parcel of the fundamental (i.e., the reactive current). Thus, simulation results are divided into two main cases. On the first case, the traditional SCS approach of the CBC is shown, and on the second, the proposed RLS methodology is evaluated. Lastly, the time response of the methodology is presented.

Initially, an overview of the system currents and voltages is presented in Fig. 3(a), comprising the SPIs turned off (named "OFF"). It is noticeable that the 2 % voltage distortion at the grid voltage triggers a resonant behavior at the PCC voltage, making a considerable amount of 3$^{rd}$, 5$^{th}$, 7$^{th}$ and 9$^{th}$ harmonic orders to be amplified, resulting in a $THD_{Vpcc}$ = 13.93 %, and a power factor (PF) of 0.411. It is reinforced that the PF is calculated herein as defined in [21]. A summary of the resulting amplitudes for the most relevant harmonic voltages, which are attained from a FFT algorithm, are shown in Fig. 3(b) for this analysis and also for the two other simulated cases. Note that, the amplitude of the fundamental component of the grid voltage, which is 179.6 $V_{peak}$, appears at the PCC being 159.2 $V_{peak}$ as a result of the trigged resonances, which comprises a voltage reduction of 12.81 % for this order.

Then, in Case 1, as depicted in Fig. 4, the CBC algorithm is enabled to perform SCS, and SPIs started sharing currents proportionally following $r_{SPIs}$ = 1.66 (i.e., $SPI_1$'s peak currents for all orders are 1.66 higher than the ones from $SPI_2$, as determined by the balanced sharing provided by the CBC methodology). As a result, although the PF increased to 0.991 and the fundamental voltage amplitude is restored to 98 % of the nominal value (i.e., 176.1 $V_{peak}$), the $THD_{Vpcc}$ slightly increased to 14.90 %. This occurred since the system presented a limited capability to distributedly damp the harmonic voltage resonances, as the power conditioners strived for the synthesis of sinusoidal currents, regardless of the highly distorted PCC voltage waveform. Matter of fact, such limitation for suppressing resonances is explicitly seen at the 5$^{th}$ harmonic in Fig. 3(b), as this order suffered a significant amplification of 7.41 times (i.e., $V_{SCS(h=5)}$ = 26.7 $V_{peak}$), in relation to the original harmonic magnitude existing at the grid voltage (i.e., $V_{PCC(h=5)}$ = 3.6 $V_{peak}$). Nonetheless, regarding harmonics other than the most significant one at the PCC voltage (i.e., 5$^{th}$ order), the SCS method is capable to efficiently damp resonances due to the distributed harmonic compensation of currents provided by the method.

In Case 2, which is shown in Fig. 5, the SPIs are able to provide the proportional current sharing of the reactive and other targeted harmonic components, while concomitantly providing more efficient

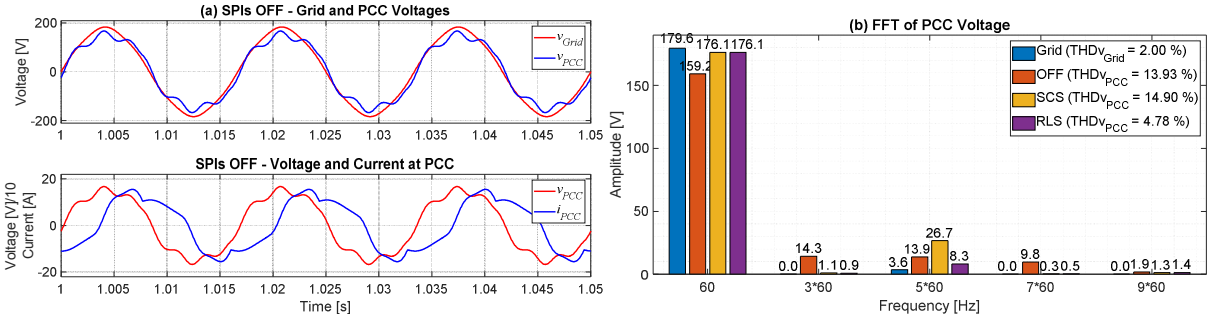


Fig. 3: Results of (a) microgrid with SPIs off (i.e., not injecting any currents), and (b) FFTs of the simulated cases.

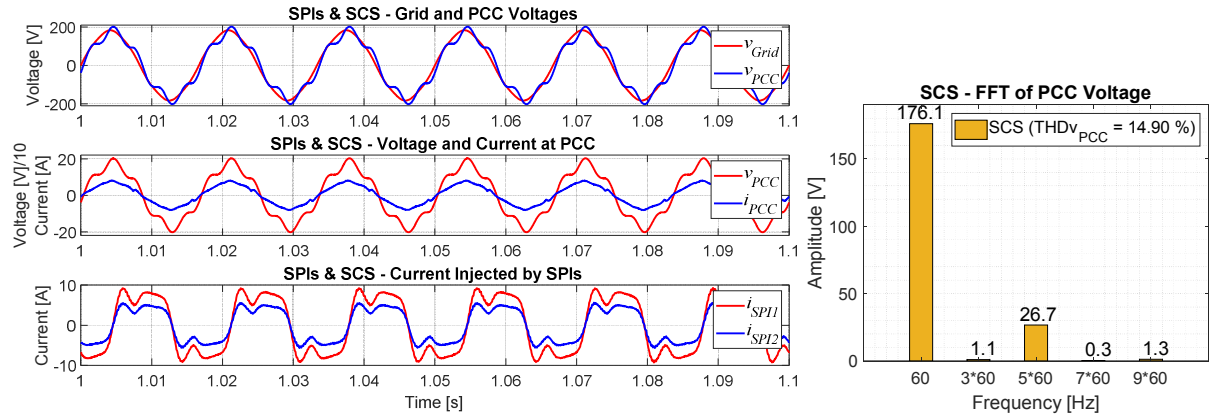


Fig. 4: Simulation results of Case 1 with SPIs performing SCS.

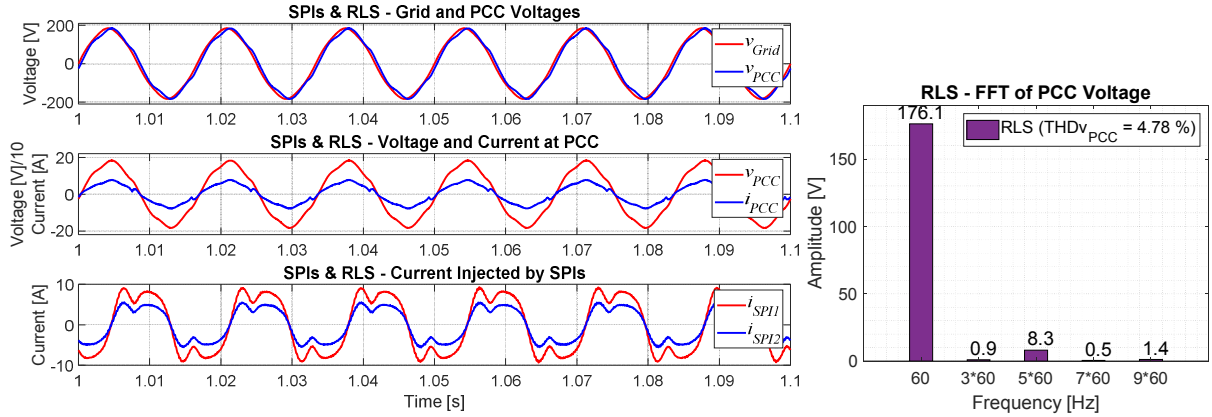


Fig. 5: Simulation results of Case 2 with SPIs performing RLS.

resonance damping, as can be noted in Fig. 3(b). This case is able to restore the amplitude of the fundamental voltage as well, reaching the same 98 % of the nominal value as the previous case. In addition, it resulted in much less distorted voltage at the PCC, presenting $THD_{Vpcc}$ = 4.78 %, which comprises a total reduction in distortion of 34.31 % in relation to the initial condition (i.e., SPIs off). Although the amplitude of the 5$^{th}$ harmonic at the PCC voltage is still 2.3 times higher than the distortion existing on the grid voltage, it remained significantly lower than on the other cases. For instance, it represents a reduction in amplitude of 1.67 times in relation to when SPIs were disabled, being also 4.42 times lower than when the CBC was performing SCS. In this case the PF increased to 0.997, and all other significant voltage harmonics (i.e., 3$^{rd}$ and 7$^{th}$) are practically damped.

Finally, Fig. 6 demonstrates the transient response of the system, showing that upon steering power conditioners to distributedly compensate undesired currents, the CBC methodology does not impose neither overcurrents on the operation of the SPIs nor overvoltages at PCC, allowing them to balance their thermal stress from the sharing of load currents. Note that, when the CBC is disabled, SPIs do not

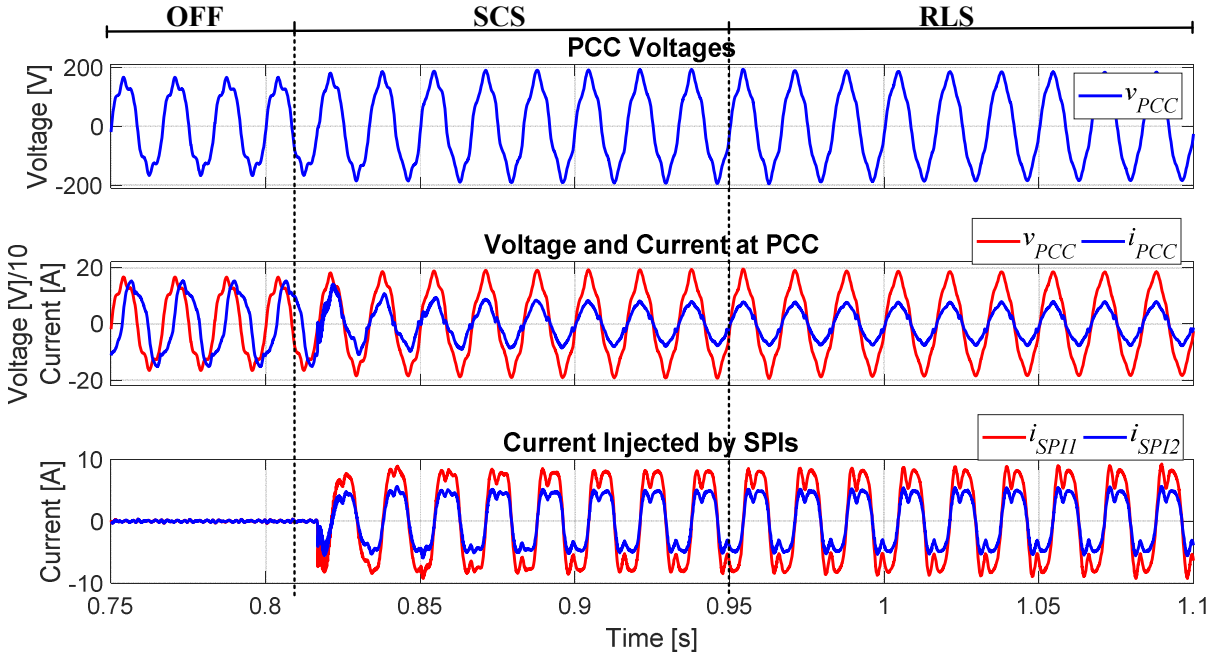


Fig. 6: Simulation results of Cases 1 and 2 considering the transient response of the CBC.

share any currents. By enabling the CBC to perform SCS in 0.81 s, since the data transmission between CC and EGs is set to occur at each fundamental cycle of the PCC voltage, the SPIs remained standing by approximately 1/4 of the cycle until current sharing began. The CBC scaling coefficients took 4 fundamental cycles to transit to a steady state condition due to the change on the PCC voltage, and the outcome of resonance amplification caused by the current injection of the SPIs. Upon adjusting the CBC algorithm to consider the RLS approach presented in this work, the SPIs adjusted their current references, and in about 3 fundamental cycles the system reached the steady state presented in Fig. 5. Note that the peak of the PCC voltage transited smoothly over the three different stages simulated.

## Conclusion

The results of this work show that, in a MG with parallel power conditioners driven as controlled current sources and operating cooperatively, there are benefits in adopting the resistive load synthesis strategy, since it provides more significant harmonic resonance damping, and consequently better power quality indices. In this work, the Current-Based Control strategy has been adopted for the coordination of the power conditioners, and as demonstrated by the simulation results, it provided smooth transition among the tested operational stages, not impairing any overvoltages or overcurrents within the MG. Yet, the strategy is able to proportionally share the currents between the SPIs according to their nominal capacities. The proposed adjustment on the classic CBC algorithm to perform RLS consisted of only changing the nodal current reference of the PCC node by the use of the Fryze's non-active current, which allowed to enhance the capability of the system to damp harmonic voltage resonances. A significant improvement in total harmonic distortion of the PCC voltage has been attained by the method, considering the capability of concomitantly coordinating SPIs to share load currents and provide distributed harmonic compensation. Future works intent to extend the method to applications in three-phase systems, demonstrating the operation of the system under more diverse and dynamic conditions of loads, while also comprising more distributed power conditioners.

## References

[1] R. C. Dugan et al, Electrical Power System Quality, McGraw-Hill, 3rd Ed. 2012.

[2] X. Liang and O. Ilochonwu, "Passive Harmonic Filter Design Scheme," *IEEE Ind. Appl. Mag.*, vol. 17, no 5, pp. 36-44, June 2011.

[3] L. H. Kocewiak, J. Hjerrild, C. L. Bak, "Wind turbine converter control interaction with complex wind farm systems", *IET Renew. Power Gen.*, vol. 7, no 4, pp. 380-389, Feb. 2013.

[4] J. He, Y. W. Li, R. Wang and C. Zhang, "Analysis and Mitigation of Resonance Propagation in Grid-Connected and Islanding Microgrids," *IEEE Trans. Energy Conv.*, vol. 30, no 1, March 2015.

[5] J. Meyer et al, "Harmonic resonances in residential low-voltage networks caused by consumer electronics," *in Proc.* 24th Int. Conf. Exhib. Electricity Distribution, June 2017.

[6] F. P. Marafao, D. I. Brandao, A. Costabeber, and H. K. M. Paredes, "Multi-task control strategy for grid-tied inverters based on conservative power theory," *IET Renew. Power Gen.*, v. 9, no. 2, pp. 154-165, Feb. 2015.

[7] T. E. Zuniga, J. A. Pomilio, "Shunt Active Power Filter Synthesizing Resistive Loads*," IEEE Trans. Power Electron.*, vol. 17, no.2, pp. 273-278, Mar. 2002.

[8] B. Meersman et al, "The Influence of Grid-connected Three-phase Inverters on Voltage Unbalance," *in Proc.* IEEE PES General Meeting, July 2010.

[9] S. Castellan, G. Buja, R. Menis, "Effective Reactive Power Compensation in Single-phase Systems Under Distorted Utility Voltage," *in Proc.* IEEE Int. SDEMPED, Oct. 2017.

[10] X. Wang, F. Blaabjerg, Z. Chen, "Autonomous Control of Inverter-Interfaced Distributed Generation Units for Harmonic Current Filtering and Resonance Damping in an Islanded Microgrid," *IEEE Trans. Ind. Appl.*, vol. 50, pp. 452-461, Jan. 2014.

[11] Y. Chen, J. M. Guerrero, Z. Shuai, Z. Chen, L. Zhou, A. Luo, "Fast Reactive Power Sharing, Circulating Current and Resonance Suppression for Parallel Inverters Using Resistive-Capacitive Output Impedance," *IEEE Trans. Power Electron.*, vol. 31, no 8, pp. 5524-5537, Aug. 2016.

[12] H. Han et al, "Review of Power Sharing Control Strategies for Islanding Operation of AC Microgrids," *IEEE Trans. Smart Grid*, vol. 7, no. 1, pp. 200-215, Jan. 2016.

[13] S. Y. M. Mousavi, A. Jalilian, M. Savaghebi, J. M Guerrero, "Autonomous Control of Current and Voltage Controlled DG Interface Inverters for Reactive Power Sharing and Harmonics Compensation in Islanded Microgrids," *IEEE Trans. Power Electron.*, vol. PP, no. 99, pp. 1-12, Jan. 2018.

[14] T. Caldognetto, S. Buso, P. Tenti, D. I. Brandao, "Power-Based Control of Low-Voltage Microgrids," *IEEE J. Emerg. Sel. Topics Power Electron.*, vol. 3, pp. 1056-1066, Dec. 2015.

[15] Z. Cheng, J. Duan, M. Chow, "To Centralize or to Distribute: That Is the Question: A Comparison of Advanced Microgrid Management Systems," *IEEE Ind. Electron. Mag.*, vol. 12, no. 1, pp. 6-24, Mar. 2018.

[16] A. M. S. Alonso, "Distributed Harmonic Compensation in Single-Phase Low-Voltage Microgrids," M.Sc. Thesis, Sao Paulo State University (UNESP), 2018.

[17] S. Fryze, "Active and Apparent Power in Circuits with Nonsinusoidal Voltage and Current," *Przegl. Elektrotech*, 1932.

[18] *IEEE Standard for Interconnection and Interoperability of Distributed Energy Resources with Associated Electric Power Systems Interfaces*, IEEE Standard 1547, 2018.

[19] M. S. Padua, S. M. Deckmann, and F. P. Marafão, "Frequency-adjustable positive sequence detector for power conditioning applications," *in Proc.* IEEE Power Electron. Spec. Conf., Recife, 2005

[20] Buso, S.; Mattavelli, P. "Digital Control in Power Electronics," 2nd Ed., Morgan&Claypool, 2015.

[21] P. Tenti, H. K. M. Paredes, P. Mattavelli, "Conservative Power Theory, a Framework to Approach Control and Accountability Issues in Smart Microgrids," *IEEE Trans. Power Electron.*, v. 26, n. 3, p. 664–673, Mar. 2011.